

An Improving Infrared Image Resolution Method via Guided Image Filtering

Wei Gan, Chao Ren, Xiaofei Wang, Xiaohai He

College of Electronics and Information Engineering, Sichuan University, Chengdu 610064

Email: DrGan2013@163.com

Abstract—Image resolution is of importance to image processing. In super resolution methods, images obtained from same sensor are adopted to improve the resolution of image. However these methods do not take advantage of the correlation of the images from different sensors to improve the resolution of image. To solve this problem, in this paper a method is proposed to enhance infrared image by using the correlation of an infrared (IR) image and its corresponding visible image. Firstly, phase congruency is used to generate the edge maps of the infrared and visible images. Then, correlated edge regions and uncorrelated regions are calculated according to the edge maps. Finally, different strategies are applied to those regions. Specifically, for the correlated regions, the visible image is considered as the guidance image while for uncorrelated regions, the infrared image itself is considered as the guidance image. Hereafter guided image filter is applied to the infrared image. Finally, the filtered result of correlated edge regions and uncorrelated regions are combined to obtain the final result. The resultant image inferred by the proposed method is with better subjective and objective quality compared with other methods.

Index Terms—infrared image processing, phase congruency, guided image filter, image enhancement

I. INTRODUCTION

Image resolution is of importance to image processing. Higher image resolution holds more details, which is important to image recognition or image segmentation. Thus, it is desired to obtain a high-resolution (HR) image from its low-resolution (LR) counterpart(s).

Due to the restrictions of the infrared capture device, infrared image resolution [1] is generally low when compared with the visible (CCD) image resolution. Thus, it is very necessary to enhance infrared image resolution by using image processing techniques.

The resolution enhancement techniques for an infrared image can be roughly classified into two categories [2-3]: image interpolation[4, 5] and image super resolution (SR) [6-11]. Image interpolation methods are the simplest methods to generate a HR image from the LR one. Generally, a resultant image by image interpolation may lack some high-frequency detail. Super resolution can generate a HR image from a LR image or a sequence of LR images. In general, SR methods have better performance compared with interpolation methods. Moreover, SR methods can be categorized into two classes, i.e. multi-frame based SR [6] and learning-based

SR [8-11]. In the multi-frame based approach, the HR image can be inferred from several sub-pixel aligned LR images while in the learning-based approach, the HR image can be derived from its corresponding LR image with an image database. Though these SR methods have good performance, these methods only adopt the correlation between the images from the same sensor. The correlation between images from different sensors is neglected.

Zomet et al.[12] used the fact that most discontinuities in the image of one sensor correspond to discontinuities in the other sensors to increase the resolution of the image from one sensor. Choi et al.[13] proposed a new framework for improving the IR image resolution by using the HR visible image information. In the framework, they adopted learning-based and reconstruction-based super resolution algorithms to improve the resolution of IR image. Park et al.[14] presented a framework to perform high quality up sampling on depth maps captured from a low-resolution 3D time-of-flight (3D-ToF) camera, which has been coupled with a high-resolution RGB camera.

Guided image filtering [15] has good edge-preserving smoothing properties, and it keeps more details than other filters. It has advantages in image enhancement and image noising[16]. Guided image filter can transfer the edge information of the guidance image into the filter output image. Usually, a visible image has more sharp edge than its corresponding infrared image. Thus, visible image could be considered as the guidance image, and its edge information can be transferred into the enhanced infrared image with guided image filter.

This paper exploits correlation between images from different sensors to enhance infrared (IR) image resolution. In particular, a novel infrared image resolution enhancement method with guided image filtering is proposed. Experimental results show that the proposed method has a good performance.

The major contributions of this paper include that 1) we adopted phase congruency to detection edge regions of infrared image and CCD images; 2) we proposed a new method to improve infrared image resolution by using guided image filtering; 3) we classified the IR image into correlated regions and uncorrelated regions. And different strategies are applied to these different regions. Taking the advantages of these contributions, the

proposed method has better performance than other methods.

The rest of the paper is organized as follows. Section II briefly reviews the guided image filtering. Correlated edge region classification is introduced in Section III. In Section IV, the detail of the approach is presented. Section V presents the results, and Section VI concludes the paper.

II. GUIDED IMAGE FILTER

The guided image filter[15] is a novel explicit image filter, which is a recently proposed edge-preserving filter. It not only has good edge-preserving smoothing properties like the bilateral filter, but also makes the filtering output more structured and keeps more details than other edge-preserving filters. Compared with the traditional edge-preserving methods, the guided image filter has advantages in image enhancement and image noising [15, 17]. In this paper, the guided image filter is first applied for improving infrared image resolution.

After applying guided image filter, the filtered output at a pixel i can be expressed as:

$$I_{out}(i) = \sum_j W_{ij}(I_c) I_{in}(j) \quad (1)$$

where I_{out}, I_{in} refer to the filtering output image and the input image respectively. i and j are the indexes of the pixels. $I_{out}(i), I_{in}(j)$ denote the gray value of the I_{out} and I_{in} at pixel i respectively. $W_{ij}(\cdot)$ denotes a filter kernel function of the guidance image I_c , and it is independent of the input image I_{in} .

The guided image filter assumes that in a local area (namely, a local window C_k , which is a square window of size $r \times r$) the relationship between the guidance image I_c and the filtering output I_{out} can be modeled by a linear transformation:

$$I_{out}(i) = a_k I_c(i) + b_k, \forall i \in C_k \quad (2)$$

where $I_c(i)$ indicates gray value of the pixel i in the guidance image I_c . a_k, b_k are the linear coefficients of the linear transformation. Herein, $i \in C_k$ denotes that pixel i is in the window C_k .

According to Eq. (2), we have $\nabla I_{out} = a \nabla I_c$, where ∇ represents the gradient. This means that the local linear transformation ensures that the filter output image I_{out} has an edge only if the guidance image I_c has an edge.

The coefficients a_k, b_k can be obtained by minimizing the following functions in the window C_k :

$$\begin{aligned} & \arg \min_{a_k, b_k} \sum_{i \in C_k} \{(I_{out}(i) - I_{in}(i))^2 + \mathcal{E} a_k^2\} \\ & = \arg \min_{a_k, b_k} \sum_{i \in C_k} \{(a_k I_c(i) + b_k - I_{in}(i))^2 + \mathcal{E} a_k^2\} \end{aligned} \quad (3)$$

where $\mathcal{E} a_k^2$ is the regularization term, \mathcal{E} is a parameter to prevent large a_k . a_k, b_k can be calculated as follows [15]:

$$a_k = \frac{\frac{1}{S} \sum_{i \in C_k} I_c(i) I_{in}(i) - \mu_k \bar{I}_k}{\sigma_k^2 + \mathcal{E}} \quad (4)$$

$$b_k = \bar{I}_k - a_k \mu_k \quad (5)$$

where μ_k and σ_k^2 are the mean and variance of the guidance image I_c in the window C_k respectively. S refers to the number of pixels in C_k . \bar{I}_k denotes the mean of I_{in} in C_k . After obtaining the linear coefficients a_k, b_k , the output I_{out} could be computed through Eq. (2).

Finally, filter kernel function in Eq. (1) can be expressed as follows

$$W_{ij}(I_c) = \sum_{(i,j) \in C_k} \left(1 + \frac{(I_c(i) - \mu_k)(I_c(j) - \mu_k)}{\sigma_k^2 + \mathcal{E}} \right) \quad (6)$$

III. CORRELATED EDGE REGION CLASSIFICATION

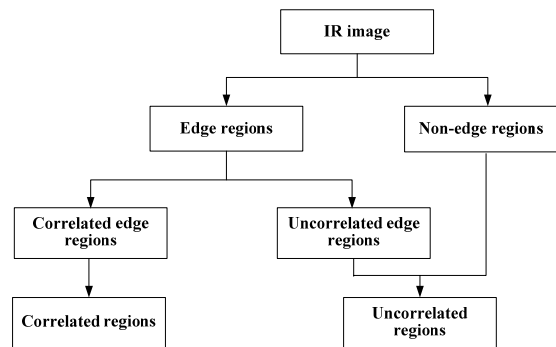


Figure 1. Diagram of the correlated regions and uncorrelated regions

Edge regions, which are very important for improving infrared image resolution, consist of high-frequency details. Thus, it is necessary to detect edges to divide infrared image into edge regions and non-edge regions. For improving infrared image resolution, our concern focuses on edge regions. However, all the edge regions in the infrared image are not correlated with their corresponding edge regions in visible image. Thus, we categorize edge regions in IR image into correlated edge region, which are correlated with their corresponding edge regions in visible image, and uncorrelated edge region, which are not correlated with their corresponding regions in the visible image. For convenience of description, the non-edge regions and the uncorrelated edge regions are called uncorrelated region, while the

correlated edge regions are called correlated regions. These correlated regions are helpful to enhance the IR image resolution, while the uncorrelated regions are useless. If these uncorrelated edge regions are used for enhancing the IR image resolution, undesirable artifacts could be introduced in the enhanced IR image. The diagram of the correlated regions and uncorrelated regions is shown in Figure 1.

A. Phase Congruency

Traditional edge detection operators, such as Sobel and Canny operator, are sensitive to noise and uneven brightness. These operators have poor performance to the infrared image. To resolve this problem, the phase congruency method[18-22] is adopted to detect infrared image edges and visible image edges to generate infrared edge maps and visible edge maps respectively.

The phase congruency is an image feature perception model, which postulates that features are perceived at points in an image where Fourier components are maximal in phase [20]. The phase congruency function of a signal I at a location x can be defined in terms of the Fourier series expansion[21]:

$$P(x) = \max_{\bar{\varphi}(x) \in [0, 2\pi]} \frac{\sum_n C_n \cos(\varphi_n(x) - \bar{\varphi}(x))}{\sum_n C_n} \quad (7)$$

where $\varphi_n(x)$ refers to the local phase of the Fourier component at x , $\bar{\varphi}(x)$ is the average phase at x , C_n represents the amplitude of the n th component in Fourier series expansion.

Calculating phase congruency needs a heavy computation load. Since the local energy functions are consistent with the phase function, local energy can be adopted to calculate phase congruency. Thus, Eq. (7) is equivalent to [21]:

$$P(x) = \frac{\sum_n C_n \cos(\varphi_n(x) - \bar{\varphi}(x))}{\sum_n C_n} = \frac{\sqrt{F^2(x) + H^2(x)}}{\sum_n C_n} \quad (8)$$

where $F(x)$ denotes the signal $I(x)$, which removes its DC component, $H(x)$ is the Hilbert transform of $F(x)$.

B. Correlated Region Classification

To obtain the correlated regions, phase congruency is performed on the infrared and visible images to generate infrared edge maps and visible edge maps respectively. Then, the normalized cross correlation is adopted to calculate the correlated edge regions. The absolute of the normalized cross correlation [12, 13] can be expressed as follows:

$$S(i) = \left| \frac{\overline{B_{VIS}(i)B_{IR}(i)} - \bar{B}_{VIS}(i)\bar{B}_{IR}(i)}}{\sqrt{(\overline{B_{VIS}^2(i)} - \bar{B}_{VIS}^2(i))(\overline{B_{IR}^2(i)} - \bar{B}_{IR}^2(i))}} \right| \quad (9)$$

where S refers to the correlation map. $S(i)$ is the absolute of the normalized cross correlation at pixel i . B_{VIS} and B_{IR} indicate the edge maps of a visible image and an infrared image respectively. And $B_{VIS}(i)$ and $B_{IR}(i)$ represent the patch centered at pixel i . $\bar{B}_{VIS}(i)$ and $\bar{B}_{IR}(i)$ denote the averages of $B_{VIS}(i)$ and $B_{IR}(i)$ respectively. The absolute of the normalized cross correlation is a good measure for similarity. The maximal absolute value of “1” indicates two signals (patches) are absolutely correlated by an affine transformation, while the minimal absolute value of “0” indicates two signals (patches) are not correlated with each other.

After generating the correlation map S , every coefficient in S above a preset threshold T is considered as a correlated pixel, which the correlated regions is composed of.

The pixel at i of the binary mask image M is set to either 1 (correlated pixel) or 0 (uncorrelated pixel, which the uncorrelated regions is composed of) according to:

$$M(i) = \begin{cases} 1, & S(i) \geq T \\ 0, & S(i) < T \end{cases} \quad (10)$$

In the binary mask image M , the pixels, whose values are 1, form correlated regions. The uncorrelated regions are composed of the pixels, whose values are 0.

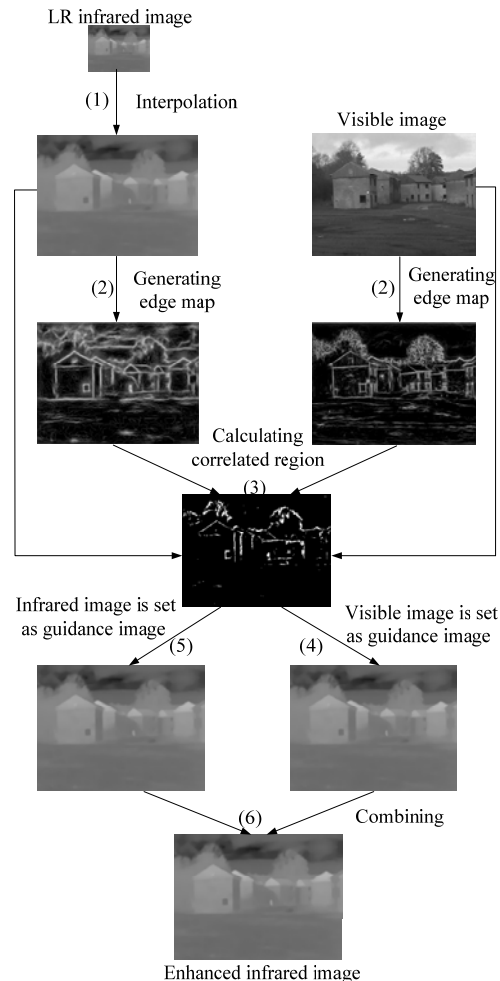


Figure 2. Flowchart of the proposed method

IV. THE PROPOSED APPROACH

After obtaining the correlated regions and uncorrelated regions, different strategies are applied to different regions. For different regions, different images are considered as guidance images. Specifically, for correlated region, visible images can be considered as the guidance image due to the correlation of infrared images and visible images. For uncorrelated region, the infrared image itself is adopted as the guidance image to enhance the infrared image to keep sharp edge and to suppress the noise because of the reason that the guided image filter has a good performance in edge-preserving and in suppressing the noise.

The framework of the proposed method is shown in Figure 2. The enhancement process is accomplished by the following steps:

- 1) Firstly, the LR infrared image is enlarged to the same size of its corresponding HR visible image with an interpolation method (Herein, we used Bicubic method).
- 2) Phase congruency is performed on the enlarged infrared image and its corresponding visible image to generate the infrared edge map and visible edge map respectively;
- 3) Correlated regions and uncorrelated regions are calculated with the edge maps by using Eq. (9) and Eq. (10).
- 4) Visible image is set as guidance image in correlated regions, and the guided image filter is performed.
- 5) Infrared image itself is set as guidance image in uncorrelated regions, and the guided image filter is performed.
- 6) The resultant images obtained in step 4 and in step 5 are combined to obtain the final enhance infrared image.

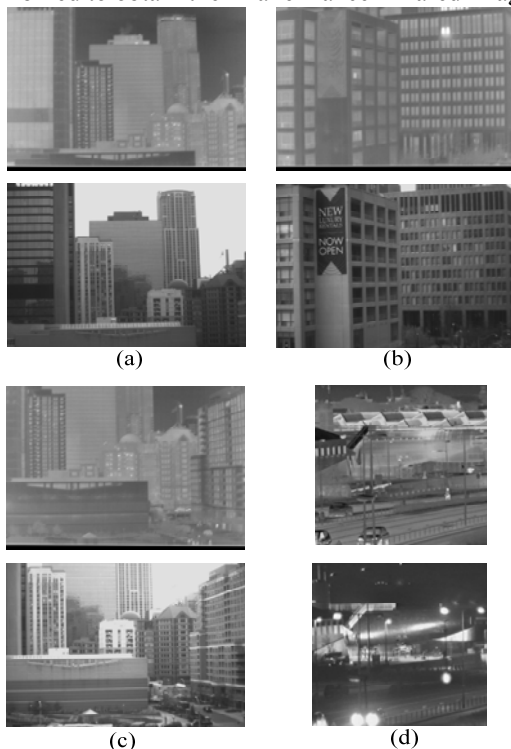


Figure 3. Four image pairs for testing (First row is the infrared image; second row is its corresponding visible image). (a) Image pair A; (b) Image pair B; (c) Image pair C; (d) Image pair D

V. EXPERIMENTAL RESULTS

We implemented our method via Matlab on a personal computer (i5-4200M 4G with 4G RAM). To evaluate the performance of the proposed method, two types of experiments are designed. The first one is to verify that the performance of phase congruency is better than that of Sobel or Canny, while the second one is for comparing the proposed method with other methods.

We employed Peak signal-to-noise ratio (PSNR) to evaluate the obtained results in terms of objective image quality assessment. The PSNR between the enhanced infrared image R and its HR reference H can be expressed as:

$$PSNR = 10 \log \frac{255^2}{\frac{1}{MN} \sum_{x=1}^M \sum_{y=1}^N [H(x, y) - R(x, y)]^2} \quad (11)$$

where $H(x, y)$ and $R(x, y)$ refer to the gray values at position (x, y) of H and R respectively. And M and N is the length and width of image. A larger PSNR indicates a better result.

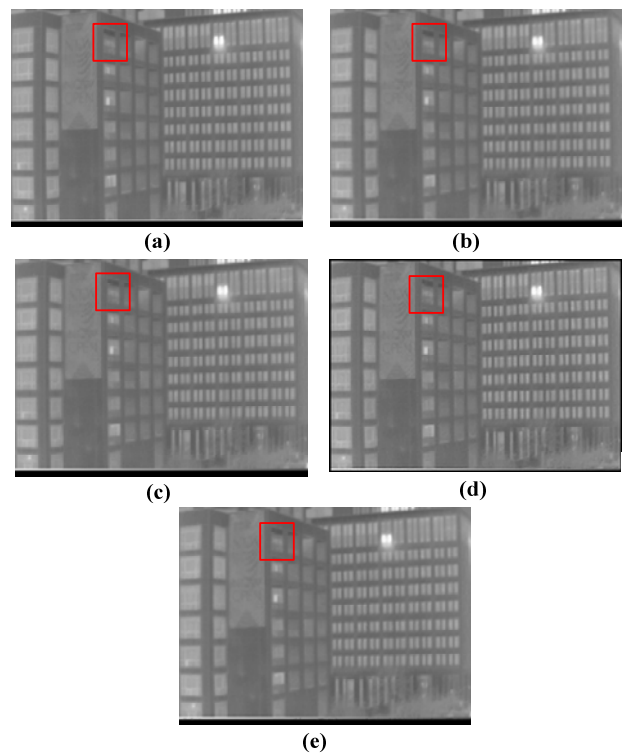


Figure 4. Experimental results of the IR image in image pair B. (a) original HR infrared image; (b) Result obtained with nearest neighbor interpolation; (c) Result obtained with Bicubic interpolation; (d) Result obtained with sparse representation based super resolution; (e) Result obtained with the proposed method

A. Experiments for the Performance of Phase Congruency

Four image pairs for testing are shown Figure 3. Each pair consists of a visible image and its corresponding infrared image. Image pairs A-C are obtained in daytime, while image pair D is got in night. In the four image pairs,

infrared images have same size with their corresponding visible images. The size of images of image pairs A-C is with 656×490 . And the size of images of image pair D is with 320×323 . All infrared images in the four pairs were down sampled to get LR infrared images. The LR infrared images are quarter-size images.

To verify that the phase congruency is better than Sobel and Canny, we compare the proposed method with Sobel or Canny based method. The Sobel or Canny based methods refer to the methods, which adopt the same steps as the proposed method except that Sobel or Canny operator rather than phase congruency are used to generate the edge maps of visible image and infrared image.

Since different regions have different characteristics, different strategies are applied to different regions. And the parameters in different regions are different. The preset threshold T is set to 0.4. In the correlated regions the visible image is used as the guidance image. Window size C_k is set to 2×2 pixels, parameter \mathcal{E} is set as 0.005^2 . In the uncorrelated regions infrared image is adopted as the guidance image. Window size C_k is 2×2 pixels, parameter \mathcal{E} is set to 0.0012.

Quantitative comparison of the performance of the deferent methods for test image pairs is given in Table I. From Table I, we can observe that the proposed method achieves best results for the four test images in terms of PSNR. The reason is that the performance of phase congruency is better than those of Sobel and Canny.

TABLE I
THE COMPARISON OF THE PERFORMANCE OF PHASE CONGRUENCY IN TERMS OF PSNR(DB)

	Image pair A	Image pair B	Image pair C	Image pair D
Sobel based method	35.50	36.04	35.44	25.48
Canny based method	35.43	36.03	35.40	25.52
proposed method	35.53	36.13	35.56	25.52

B. Experiments for Comparing the Proposed Method with Other Methods

This subsection is for comparing the proposed method with other methods. And two types of experiments are designed. The first one deals with common infrared images. The second one is for noisy infrared images to further validate the proposed method. In experiments, we considered other three methods for comparison: nearest-neighbor interpolation, Bicubic interpolation, sparse representation based super resolution [9].

The same test images used in previous subsection are used in this subsection. Figure 4 shows the experimental results of the IR image for image pair B. We can observe that the result of nearest neighbor interpolation and Bicubic interpolation blur the most image detail in Figure 4(b)-(c). Sparse representation based method can restore some high-frequency details in Figure 4(d). However it contains some artifacts. There is no obvious artifact available in the results obtained with the proposed

method. For further comparison, Figure 5 shows a zoomed version of the marked region in Figure 4.

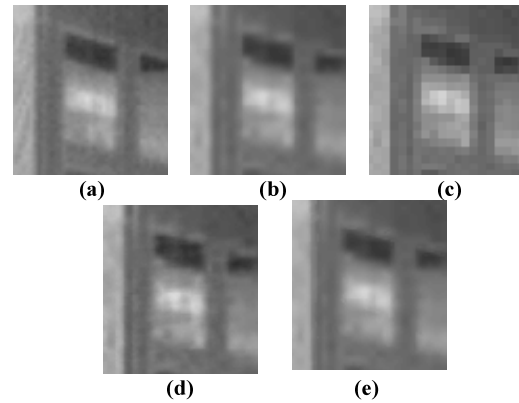


Figure 5. The zoomed version of the labeled region of Figure 3. (a)–(e) the zoomed version of the labeled area of (a)–(e) in Figure 3

Quantitative comparison of the performance of the deferent methods for test image pairs is given in Table II. From Table II, we can observe that the proposed method achieves best results for the four test images in terms of PSNR. Also it can be observed that the quantitative metric coincides with the above visual effect very well. We can draw the conclusion that the proposed method is with higher performance when compared with other methods.

TABLE II
THE COMPARISON OF THE PERFORMANCES OF DIFFERENT METHODS IN TERMS OF PSNR(DB)

	Image pair A	Image pair B	Image pair C	Image pair D
Bicubic interpolation	35.42	36.02	35.50	25.52
Nearest neighbor interpolation	33.29	33.00	33.33	23.80
Sparse representation based super resolution	35.65	34.27	35.25	24.05
Proposed method	35.53	36.13	35.56	25.52

To further validate the proposed method, this experiment deals with noisy infrared image. We artificially added zero mean white Gaussian noise with standard deviation 0.5 to the LR infrared images, which are used as test image in previous section, to produce noisy infrared images.

Due to the noise in the infrared image, the window size is set to bigger size, i.e. 4×4 pixels to suppress the noise. The parameter of \mathcal{E} is 0.1^2 .

Figure 6 illustrates an example of the resultant images of image pair D by using different methods. Figure 7(a)-(d) show the zoomed versions of the labeled region in Figure 6(b)-(e).

It can be seen that the results of nearest neighbor interpolation, Bicubic interpolation, and sparse representation based method are seriously affected by noise. The proposed method can achieve better results than interpolation methods and sparse representation based method. The results obtained with the proposed methods are free from such artifacts. The details of the results of the proposed methods can be observed.

TABLE III
THE COMPARISON OF THE PERFORMANCES OF DIFFERENT METHODS
FOR NOISY IMAGE IN TERMS OF PSNR(DB)

	Image pair A	Image pair B	Image pair C	Image pair D
Bicubic interpolation	25.58	25.63	25.65	23.00
Nearest neighbor interpolation	23.69	23.65	23.77	21.19
Sparse representation based super resolution	21.71	21.73	21.76	21.19
Proposed method	30.41	29.84	30.32	24.18

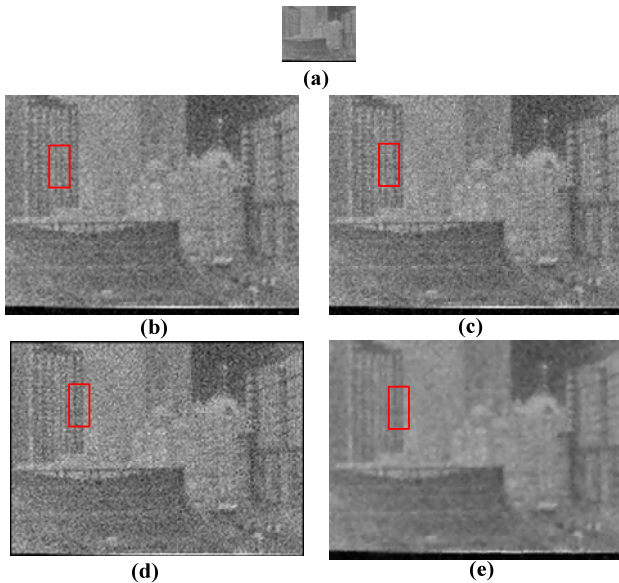


Figure 6. Experimental results of the noisy IR image in image pair C (a) noisy LR infrared image; (b) Result obtained with nearest neighbor interpolation; (c) Result obtained with Bicubic interpolation; (d) Result obtained with sparse representation based super resolution; (e) Result obtained with the proposed method

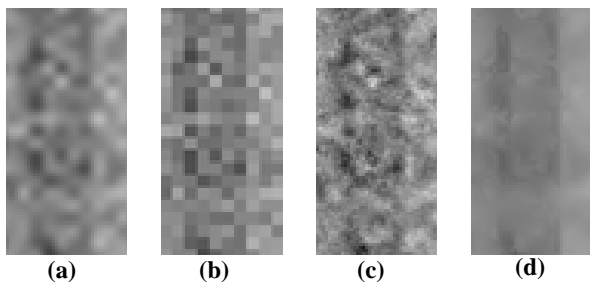


Figure 7. The zoomed version of the labeled region of Figure 5. (a)-(d) the zoomed version of the labeled area of (b)-(e) in Figure 5.

Table III lists a comparison of results of different methods on objective evaluation in terms of PSNR. From Table III, we can observe that the performance of the proposed method is better than those of other methods in terms of PSNR. The proposed method can work well on the infrared image or the noisy infrared image.

VI. DISCUSSION AND CONCLUSION

Traditional super resolution methods enhance the image resolution by using the correlated information between images from a same sensor. Different with traditional super resolution, we exploit to enhance the infrared image resolution using the correlation between

two different types of images from different sensors. Thus, this paper proposes a method to enhance resolution of infrared images by guided image filter. The most important contributions of this paper consist of two points. Firstly, a new method is proposed to improve infrared image resolution by using guided image filtering. Secondly, different strategies are proposed to apply to correlated regions and uncorrelated regions. Experimental results demonstrate a good performance of the proposed method in terms of subjective visual and PSNR in comparison with some state-of-the-art techniques.

The time complexity of the proposed method depends on three steps i.e. step 2, 3 and step 4 of the proposed method as shown in Figure 3. For step 2, computation of phase congruency is very costly. For step 3, only edge regions, which are only a small part of the image, are processed. Thus, this step has a low complexity. For step 4, the guided filter has an $O(N)$ time operations, where N refers to the pixels of the processed image. Based on above analysis, the time complexity of the proposed method depends on the time complexity of phase congruency.

The reasons, that guided image filtering works well for improving IR resolution, consists of that 1) visible image has more details (sharp gradient) than infrared image; and 2) guided image filter can transfer gradient of the guidance image I_c into the filter output image I_{out} . In other words, guided image filter can transfer gradient of the visible image into the infrared image, if we consider visible image and infrared image as the guidance image and the filter output image respectively. Generally, the model for guided image filter is very useful to improve infrared image resolution by using visible image.

The limitations of the proposed method include that 1) the proposed method has a high time complexity since computation of phase congruency is very costly; 2) the proposed method is sensitive to some parameters, e.g. patch size. For the future work, the proposed method can be further improved by exploiting other edge detection methods rather than phase congruency. Other improvement is to automatically choose a size instead of a fixed size for a patch to achieve good performance.

ACKNOWLEDGMENT

This work is supported by National Natural Science Foundation of China under Grant No. 61071161, Joint Fund of the National Natural Science Foundation of China and the China Academy of Engineering Physics No. 11176018.

REFERENCES

- [1] A. Zhu, Y. Li, L. Lv, H. Zhang. "Dual-Module Data Fusion of Infrared and Radar for Track Before Detect", Journal of Computers, vol. 7, no. 12, pp.2861-2867, 2012.
- [2] S.C. Park, M.K. Park, M.G. Kang. "Super-resolution image reconstruction: a technical overview", IEEE Signal Processing Magazine, vol. 20, no. 3, pp. 21- 36, 2003.
- [3] J.D. Van. "Image super-resolution survey image super resolution survey", Image and Vision Computing, vol. 24, no. 10, pp. 1039- 1052, 2006.

- [4] X. Zhang, X. Wu. "Image interpolation by adaptive 2-D autogressive modeling and soft decision estimation", IEEE Transaction Image Processing, vol. 17, no. 6, pp. 887-896, 2008.
- [5] K. Guo, X. Yang, H. Zha, W. Lin, S. Yu. "Multiscale semilocal interpolation with antialiasing", IEEE Trans Image Process, vol. 21, no. 2, pp. 615-625, 2012.
- [6] P. Antogni, A. Vassilis. "Super-Resolution Reconstruction of Thermal Infrared Images". Proceeding of the 4th WSEAS International Conference on Remote Sensing, pp40-44, 2008.
- [7] F. Qin, L. Zhu, L. Cao, W. Yang. "Blind Single-Image Super Resolution Reconstruction with Gaussian Blur and Pepper & Salt Noise", Journal of Computers, vol. 9, no.4, pp. 896-902, 2014.
- [8] W. Wu, Z. Liu, X. He. "Learning-based super resolution using kernel partial least squares", Image and Vision Computing, vol. 29, no. 6, pp. 394-406, 2011.
- [9] J. Yang, J. Wright, T. S. Huang et al. "Image Super-Resolution Via Sparse Representation", IEEE Transactions on Image Processing, vol. 19, no. 11, pp. 2861-2873, 2010.
- [10] K. Ni, Q.N. Truong. "Image superresolution using support vector regression", IEEE Transactions on Image Processing, vol. 16, no. 6, pp.1596-1610, 2007.
- [11] C.V. Jiji, S. Chaudhuri. "Single-frame images super-resolution through contour learning", EURASIP Journal on Applied Signal Processing, 2006, pp.1-11, 2006.
- [12] R. Zhu, Y. Wang, E. Sneekenes. "Application of Improved Median Filter on Image Processing", Journal of Computers, vol. 7, no.4, pp.838-841, 2012.
- [13] K. He, J. Sun, X. Tang. "Guided image filtering". IEEE Transactions on Pattern Analysis and Machine Intelligence. vol.35, no.6, pp.1397-409, 2013.
- [14] S. Li; X. Kang; J. Hu. "Image Fusion With Guided Filtering", IEEE Transactions on Image Processing, vol. 22, no.7, pp.2864-2875, 2013.
- [15] W. Chen, Y. Shi, W. Su. "Image splicing detection using 2-D phase congruency and statistical moments of characteristic function", Security, Steganography, and Watermarking of Multimedia Contents IX 2, 1-8, 2007.
- [16] M.C Morronea, R.A.Owens. "Feature detection from local energy", University of Western Australia, Nedlands, 2003.
- [17] Z. Liu, R. Laganiere. "Phase congruence measurement for image similarity assessment", Pattern Recognition Letters, vol.28, no.1, pp.166-172, 2007.
- [18] C. Li, A. C. Bovik, X. Wu. "Blind Image Quality Assessment Using a General Regression Neural Network", IEEE Transactions on Neural Networks, vol.22, no.5, pp.793-799, 2011.
- [19] L. Zhang, L. Zhang, X. Mou, D. Zhang. "FSIM: A Feature Similarity Index for Image Quality Assessment", vol.20, no.8, pp.2378-2386, 2011.
- [20] A. Zomet, S. Peleg. "Multi-sensor Super Resolution", Proceeding of the Sixth IEEE Workshop on Applications of Computer Vision, pp.27-31, 2002.
- [21] K. Choi, C. Kim, M. Kang et al. "Resolution Improvement of Infrared Images Using Visible Image Information", IEEE Signal Processing Letters, vol.18, no.10, pp.611-614, 2011.
- [22] J. Park, H. Kim, Y. Tai. "High quality depth map upsampling for 3D-TOF cameras", IEEE International Conference on Computer Vision (ICCV), 1pp.623-1630, 2011.